Stability of carbon nanotubes under electron irradiation: Role of tube diameter and chirality

A. V. Krasheninnikov,[1,2] F. Banhart,[3] J. X. Li,[3] A. S. Foster,[1] and R. M. Nieminen[1]
[1]*Laboratory of Physics, Helsinki University of Technology, P.O. Box 1100, Helsinki 02015, Finland*
[2]*Accelerator Laboratory, P.O. Box 43, FIN-00014 University of Helsinki, Finland*
[3]*Institut für Physikalische Chemie, Universität Mainz, D-55099 Mainz, Germany*
(Received 21 June 2005; revised manuscript received 14 July 2005; published 22 September 2005)

As recent experiments demonstrate, the inner shells of multiwalled carbon nanotubes are more sensitive to electron irradiation than the outer shells. To understand the origin of such counterintuitive behavior, we employ a density-functional-theory based tight-binding method and calculate the displacement threshold energies for carbon atoms in single-walled nanotubes with different diameters and chiralities. We show that the displacement energy and the defect production rate strongly depend on the diameter of the nanotube and its chirality, with the displacement energy being lower, but saturating towards the value for graphite when the tube diameter increases. This implies that the threshold electron energies to produce damage in nanotubes with diameters smaller than 1 nm are less than the commonly accepted value for graphitic nanoparticles. We also calculate the displacement energies for carbon atoms near defects and show that if a single vacancy is formed, it will likely be transformed to a double vacancy, as the nanotube atomic network with double vacancies has no energetically unfavorable undercoordinated atoms.

DOI: 10.1103/PhysRevB.72.125428 PACS number(s): 61.46.+w, 61.80.Az, 68.37.Lp

I. INTRODUCTION

Electron irradiation of carbon nanotubes has proved to be an outstanding example of nanoengineering. In modern electron microscopes with field emission guns, the electron beam can be focused onto areas of several Å. This allows one to selectively modify nanostructures on an atomic scale by displacing or removing atoms from pre-defined regions. Carbon nanotubes are particularly suited for beam-induced nanomanipulation since the graphitic network has a high tendency to re-arrange after the formation of point defects. For example, welding[1] and coalescence[2] of carbon nanotubes by the electron beam have been demonstrated, which opens a different way for making a network of connected nanotubes for material reinforcement and use in nanoelectronics. The mechanical properties of nanotube bundles,[3] and in principle macroscopic nanotube samples,[4] can be improved due to intertube links produced by electron irradiation.

The irradiation-induced structural transformations in single-walled and multiwalled nanotubes (SWNTs/MWNTs) are due to the defects, mostly vacancies and interstitials, created by the impacts of energetic electrons followed by saturation of highly reactive dangling bonds at undercoordinated carbon atoms. Thus knowing the defect production mechanism and how the defect production rate is related to the beam characteristics is extremely important for controlling the transformations. Moreover, as carbon nanotubes are routinely characterized nowadays in the transmission electron microscope (TEM), the complete understanding of the interaction of energetic electrons with nanotubes should also minimize the amount of damage when it is an undesirable side effect.

Several TEM studies on irradiation-induced defects in carbon nanotubes have already been carried out.[5–13] Early experiments[5] showed that SWNTs exposed to focused electron irradiation were locally deformed and developed necklike features due to removal of carbon atoms by knock-on displacements. Uniform irradiation of SWNTs (Ref. 9) resulted in surface reconstructions and drastic dimensional changes, as a corollary of which the apparent diameter of the nanotubes decreased from 1.4 to 0.4 nm. Experimental and theoretical studies also demonstrated that the electron beam creates defects nonuniformly: carbon atoms are most rapidly removed from surfaces lying normal to the beam direction.[6,10]

Very recently, it has been shown experimentally[13] that MWNTs subjected to electron irradiation are destroyed from inside and that it is the inner shell which collapses first. Concurrently with these experiments, qualitatively similar results[12] were obtained for double-walled nanotubes at different temperatures.

It has been demonstrated[13] that a lower stability of the inner shells is due to a combination of two effects: a higher defect production rate in the inner shells and fast migration of carbon interstitials via the inner hollow in the axial direction. The defect production rate is related to the tube diameter, as the displacement threshold is lower for thin nanotubes with highly curved atomic network.

In this work, we theoretically study the relationship between the tube diameter and displacement rate in more detail. We also address the role of chirality. Finally, to better understand the evolution of nanotubes under high-dose irradiation, we calculate the displacement energies for carbon atoms near defects which can exist in nanotubes or appear due to interaction with the electron beam.

II. EVOLUTION OF MWNTs UNDER HIGH-DOSE ELECTRON IRRADIATION: TEM EXPERIMENTS

Similar to recent experiments,[13] MWNTs were exposed to an intense focused electron beam in a TEM (FEI Tecnai F-30) with field emission electron gun operating at 300 kV. To prevent the agglomeration of interstitial atoms,[8] the speci-

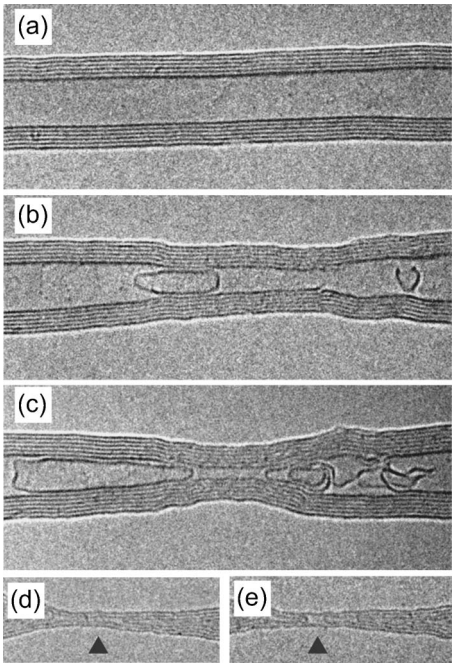

FIG. 1. Morphological evolution of a multiwalled carbon nanotube under electron irradiation. An electron beam with 300 keV and beam current density of approximately 450 A/cm was focused onto an area of 10–20 nm over the central part of the tube. The sequence (a)–(e) shows the evolution of a typical tube during some minutes of irradiation. In (d) and (e) only two shells or one shell are left, respectively. Specimen temperature: 600 °C. The solid arrows indicate the position of the beam center where the shells successively break.

mens were held at temperatures around 600 °C in a heating stage. Small sections of the tubes were exposed to an electron beam of 10–25 nm in diameter at beam current densities of 60–500 A/cm^2.

Figure 1 shows an example of the collapse of a MWNT under the electron beam. As seen in Figs. 1(b) and 1(c), aggregates of material in the shape of irregular graphitic cages occurs in the hollow core. While all shells shrink, the outer shells remain undamaged, but the inner shells are successively lost until a single-wall tube in the center is left, see Figs. 1(d) and 1(e). After breakage of the innermost layer, the two halves form cones with closed caps which slowly retract in the axial direction.

The lower stability of the inner shells, which can be clearly deduced from the observations, can be due to a higher rate of defect generation in the inner shells and/or a higher diffusivity of the defects in the inner hollow of the tube. Some interstitial-vacancy pairs anneal *in situ* and thus enhance the resistivity of the tubes to irradiation, especially at temperatures above 300 °C, as previous experiments indicate.[12,14] However, even if the behavior of the irradiated tubes is governed by diffusion (e.g., at high temperatures), the defect production rate is a very important factor.

To some extent, the lower stability of inner shells is a counterintuitive result, as carbon atoms displaced from the inner shells remain inside the tube making recombination possible, while the atoms sputtered from the outer shells leave the tube. Thus one can expect that the outer shell should be less stable and develop cracks and big vacancy clusters during irradiation. However, this is not observed.

III. COMPUTATIONAL DETAILS

To understand the effect of chirality and shell diameter, i.e., the curvature of the carbon network, on the defect production rate, we employed molecular-dynamics methods with the nonorthogonal density-functional based tight-binding (DFTB) force model[15,16] to describe the interaction of C atoms at the quantum-mechanical level. As shells in MWNTs weakly interact with each other, we can consider collisions of energetic electrons with individual shells to estimate the curvature effects on the displacement energy. Due to a large separation between the shells, the trajectory of the recoil atom just after the electron impact should be roughly the same independent of whether other shells are present or not. Obviously, when the atom displacement is large, the recoil atom in MWNTs start interacting with other shells, which should affect the atom trajectory and thus the displacement energy. However, with respect to the effect of curvature, the qualitative behavior should be the same in SWNTs and MWNTs.

It is well known[6,14] that the primary cause of the electron irradiation damage in nanotubes are knock-on collisions of electrons with atomic nuclei. The collision time is very short as compared to the characteristic times of the atomic motion.[14] Thus, to get insight into defect production, we can assume that a carbon recoil atom instantaneously acquires some kinetic energy due to a collision and then treat the motion of atoms adiabatically.

Our previous DFTB calculations of formation energies of interstitial-type defects in carbon nanotubes showed a good agreement between the results obtained with DFTB and *ab initio* calculations.[17] To further test our model for vacancy-type defects, we evaluated the vacancy formation energy E_v for a flat graphene flake. We found that $E_v=7.6$ eV, which is in very good agreement with a first-principle result of 7.7 eV.[18] To have a reference point for a strongly curved system, we calculated E_v for a (4,4) nanotube with DFTB and plane-wave (PW) DFT code VASP.[19] The results proved to be in excellent agreement: 5.34 eV vs 5.31 eV (DFTB/PW DFT). We also evaluated E_v for SWNTs as a function of tube diameter. We found that the curvature gave rise to a decrease in the vacancy formation energy: $E_v=6.8$ eV for a (12,12) SWNT, $E_v=4.4$ eV for a (3,3) SWNT, which is also in a good agreement with the published data.[20]

Simulations were carried out for armchair and zigzag SWNTs composed of 80–320 atoms and with diameters of from 4 to 17 Å and length of 12–13 Å. Periodic boundary conditions along the tube axis were used. Test calculations for longer nanotubes gave essentially the same results.

IV. RESULTS AND DISCUSSION

Having tested our model, we calculated the displacement energy T_d for graphite and nanotubes in two different ways. First, we evaluated T_d by running free molecular dynamics,

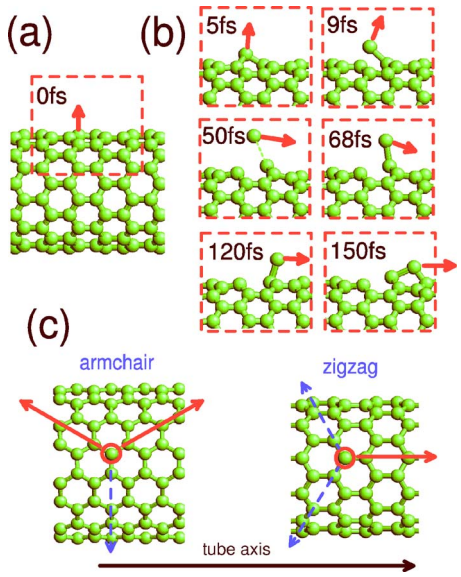

FIG. 2. (Color online) (a) The simulation setup used (side view). (b) Several snapshots showing the atom positions after electron impact onto a zigzag nanotube. The initial energy of the recoil atom is just above the threshold for defect production. (c) The atomic networks of armchair and zigzag nanotubes (top view). The arrows show the most probable directions of the recoil atom motion (projection to the tube surface) when the original recoil atom velocity is perpendicular to the tube surface.

as in Ref. 6. Then we estimated T_d statically, assuming that T_d is related to the formation energy of the interstitial-vacancy (i-v) pair E_{iv}.

A. Dynamical calculations of the displacement energy

In our dynamical simulations, we assigned a kinetic energy to a carbon atom (the recoil atom) in the graphene or nanotube network and simulated the evolution of the system by running free molecular dynamics. The initial momentum vector was perpendicular to the graphene-nanotube surface, as such a configuration corresponds to the smallest escape energy.[6] Figure 2(a) shows our simulation setup.

At low initial energies of the recoil atom none of the three bonds are broken and the kinetic energy transmitted to the atom by the electron is redistributed among other atoms in the system in accordance with the equipartition theorem, thus heating up the system.[21] When the energy increases, one or two bonds are broken, but the recoil atom does not go far from its original position and immediately recombines with the vacancy. The recombination can be complete, with the restoration of the perfect arrangement of carbon atoms in the graphitic network, or incomplete—in many cases we observed formations of metastable Stone-Wales defects.[22] The appearance of these defects is not surprising as the energy brought into the system by the energetic electron is much larger than the activation barrier (6–8 eV) for the defect formation.[23,24] These topological defects representing a pentagon-heptagon pair are metastable, at least at low temperatures, and can be detected by spectroscopic techniques.[25] At high initial energies the recoil atom leaves its position and

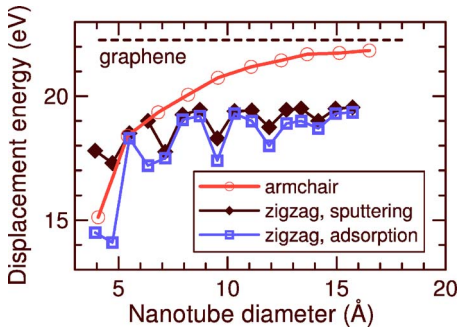

FIG. 3. (Color online) Threshold energy T_d needed to displace a carbon atom from armchair and zigzag single-walled carbon nanotubes and graphene calculated dynamically as a function of tube diameter. The solid lines are guides for the eye.

travels to infinity or it is adsorbed on the tube surface outside the immediate recombination radius, as depicted in Fig. 2(b).

We defined T_d as the minimum initial kinetic energy of a C atom to leave its position in the nanotube atomic network and not recombine before the energy is re-distributed among the other atoms in the system. In practice, we ran simulations for 1 ps. Although this simulation time was too short to guarantee the Maxwellian distribution of atom velocities, the maximum kinetic energy of any atom after the run did not exceed 0.2 eV, so that immediate recombination was unlikely. Longer test runs (5 ps) gave the same results. Surely the defects can recombine due to thermal diffusion on a longer time scale, but this is a different effect.

We found that $T_d \approx 22$ eV for graphene. This is in line but somewhat larger than the values of 15–20 eV reported in experimental studies[14] for graphite. However, we would like to stress that the calculated value of T_d is the *upper bound* on T_d; in reality T_d is somewhat smaller due to minor thermal fluctuations and electronic effects lowering the potential barriers.

T_d as a function of tube diameter for armchair SWNTs with chiral indices spanning from 3 to 12 and zigzag tubes with indices from 5 to 20 is presented in Fig. 3. It is evident that T_d decreases as the tube diameter is getting smaller with the difference between graphene and the smallest armchair SWNT considered being about 7 eV.

For zigzag nanotubes the qualitative picture was similar. However, there are several features different from the armchair tube behavior. We found that the initial atom energy needed for the atom to travel to infinity (curve labeled "sputtering" in Fig. 3) was different from the atom energy to leave its position and get stuck on the same tube (curve "adsorption" in Fig. 3). The difference was small for armchair tubes, but substantial for zigzag nanotubes, especially those with small diameters. The reason for that is the orientation of the graphitic network with respect to the tube axis and two types of bonds (oriented perpendicular and parallel to the tube axis). The "perpendicular" bond is strained due to the curvature. Thus it is easier to break these bonds, so that the atom velocity acquires a component along the "strong" bond, see Fig. 2(c). In zigzag tubes this direction coincides with the tube axis, that is why the recoil atom has a higher probability for adsorption. In armchair tubes the recoil atom velocity

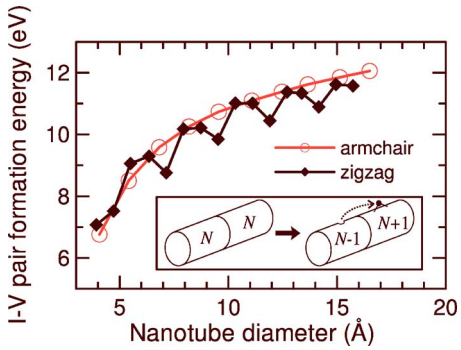

FIG. 4. (Color online) Formation energy of an interstitial-vacancy pair in carbon nanotubes as a function of tube diameter. The lines are guides for the eye. The inset schematically shows the simulation setup used to calculate the formation energy.

always has a component perpendicular to the tube axis, thus decreasing the adsorption probability.

Different orientations of the network may also explain why T_d is smaller for zigzag tubes than for armchair SWNTs of the same diameter. In zigzag tubes, there are two strained bonds, while in armchair tubes only one bond is strained. Besides this, the vacancy formation energy in a zigzag SWNT is lower than that for an armchair nanotube with the same diameter.[20] The dependence of the total electron energy on the system length may also affect the results, although, as mentioned above, test calculations for longer tubes gave very close results (the difference was less than 0.1 eV). However, the effect of network orientation should be weaker when the initial recoil velocity direction is random. Thus one can expect that the difference between armchair and zigzag nanotubes should be smaller for SWNTs/MWNT shells with diameters over 2 nm and vanish for the outer shells in the typical MWNTs.

Another interesting effect is a saw-tooth shape of the curve. The oscillations are related to the electronic structure of zigzag nanotubes.[20] The local minima on the curve correspond to the nanotubes with chiral indices 6, 9, 12, etc., which are metallic, while all the other tubes are narrow-band semiconductors. Note that oscillations are absent for armchair SWNTs which are always metallic.

B. Static calculations of the displacement energy

In the second simulation setup, we assumed that T_d is related to the formation energy of the interstitial-vacancy (i-v) pair E_{iv} and calculated E_{iv} statically as

$$E_{iv} = E(N+1) + E(N-1) - 2E(N), \tag{1}$$

where $E(N+1)$ is the total energy of the system with a carbon adatom, $E(N-1)$ is the energy of the system with a vacancy, $E(N)$ stands for the energy of the perfect system composed of N atoms; see also the inset in Fig. 4. Recall that due to empty space in nanotube samples, adatoms play the role of interstitials in SWNTs samples.[26] Note also that Eq. (1) does not account for the barrier separating the ideal and defect configurations, so that it provides information on the *lower bound* on T_d.

Static calculations for graphene gave $E_{iv} \approx 15$ eV. This agrees with the experimental data, being on the lower side of the scatter of the data. The dependence of E_{iv} on the tube diameter is shown in Fig. 4. Similar to the results obtained in the dynamical approach, E_{iv} is much less for tubes with small diameters. The difference between graphene and marginally stable SWNTs also proved to be about 7 eV.

One can expect that the actual value of T_d is between the upper and the lower bounds. However, the most important result is that, no matter what the absolute value of T_d for a given graphitic structure is, finite curvature gives rise to a substantial drop in T_d. Thus the electron threshold energy for displacing a carbon atom should be lower for SWNTs with small diameters and, correspondingly, for inner shells of the MWNTs.

The drop in T_d is due to two factors: the strain in the carbon network and the ability of the nanotube to reconstruct by saturating dangling bonds. It is intuitively clear that it is easier to displace the atom when the carbon network is strained and thus the absolute value of the cohesive energy is smaller. However, the difference in the cohesive energy between graphite and small diameter nanotubes is very small, about 0.4 eV per atom, and this alone cannot explain the difference of about 7 eV in T_d and E_{iv}.

However, as simulations indicate, it costs much less energy to create a vacancy in a nanotube with small diameter than in graphite.[20] Physically, this is due to the ability of the curved nanotube network to reconstruct more efficiently than for flat graphite, so that the mechanical strain in the atomic network resulting from dangling bond saturation is lower. Note that T_d is related to E_{iv}, while the latter can be represented as a sum of the vacancy and adatom formation energies, $E_{iv}=E_v+E_{adatom}$. Thus smaller values of T_d originate from the nanoscale size of carbon nanotubes and the unique shape of their atomic network.

C. Evaluation of the displacement cross section

Different values of T_d point to different displacement cross sections, i.e., how frequently the atoms are displaced during the irradiation. We calculated the displacement cross section by applying the McKinley-Feshbach formalism.[27] We assumed the qualitative behavior of T_d as shown in Figs. 3 and 4 and a displacement threshold of $T_d=15-17$ eV for graphite, which might be a realistic value. Hence we could evaluate the displacement rate for nanotubes with different diameters. Calculations show that the cross-section in a (3,3) tube would be higher by almost a factor of 2 than in nanotubes with diameters over 2 nm. Thus the displacement rate is higher for the atoms in the inner shells than for the atoms in the outer shells; this is in accordance with the experimental results.

The lower values of T_d correspond to lower electron energies E^e_{kin}, or correspondingly, to lower voltages in the TEM. Within the binary collision approximation,[14] $T_d=15$ eV gives $E^e_{kin} \sim 82$ keV, which is very close to the experimental values of the threshold electron energy (86 keV) (Ref. 10) reported for SWNTs with diameters apparently exceeding 1 nm (the diameters were not specified in that work). However, if the

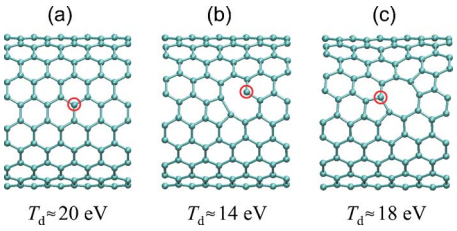

FIG. 5. (Color online) The atomic network of a (8,8) armchair nanotube and the energies needed to knock out the atom (marked with a circle) from the intact tube (a), nanotube with a vacancy (b), and a double vacancy (c).

nanotube diameter is under 1 nm, the electron energy should be much lower, e.g., $T_d = 12$ eV corresponds to $E^e_{kin} = 66$ keV. The lower values for thin nanotubes can explain the drastic changes in the mechanical properties of irradiated nanotube bundles[3] (presumably due to irradiation-induced covalent bonds between individual tubes) at irradiation energies below the threshold value, as nanotubes with smaller diameters may be present in the bundles. We would also like to point out that electrons with low energies can create damage to nanotubes by stimulating chemical reactions when impurities are present,[28] but knock-on damaging mechanism works even for perfectly clean nanotubes.

D. Interaction of the electron beam with defected nanotubes

Another important factor which may affect the evolution of nanotubes under irradiation, is the response of a nanotube with defects to the irradiation. Assuming that a single vacancy had been already formed, we calculated the energy T^v_d needed to displace the dangling bond atom, Fig. 5(b). T^v_d proved to be 13–14 eV and only weakly dependent on the tube diameter. The physical reason for the drop in the energy is the necessity to break two bonds instead of three. Hence a double vacancy can easily be formed, as a drop in the displacement energy should result in an increase in the cross section.

The double vacancy defects are particularly stable in nanotubes,[29–31] as no atom with dangling bonds is present in the atomic network. This also gives rise to an increase in the threshold energy (16–18 eV) needed to create a trivacancy. Lower values (as compared to the perfect tube) are due to pentagons and octagons in the network, and thus lower local bonding energies.

Double vacancies in nanotubes can result in further structural transformations, such as local buckling, diameter reduction, and local re-arrangement of the atomic network, but these changes would require high temperatures to overcome high-energy barriers separating the configurations. Thus it is very probable that point defects observed in recent TEM experiments[11,12] are double vacancies.

Note also that coalescence of single vacancies into double vacancies is energetically favorable, as the latter have no dangling bond. Thus the number of double vacancies can increase due to vacancy coalescence. Presence of double vacancies in irradiated nanotubes was corroborated by recent experiments on the dependence of the SWNT conductance on Ar ion irradiation dose.[32]

The other factor which affects the evolution of nanotubes under irradiation is the diffusivity of interstitials. As we recently showed,[17] carbon atoms can easily migrate via the inner hollow. Our recent experimental studies[33] seem to confirm this prediction. Thus, at elevated temperatures, the stability of nanotubes may be governed by diffusion. However, the displacement rate should be close to that at low temperatures, as the threshold energy is the same.[6]

V. CONCLUSIONS

By employing a density-functional-theory based tight-binding method we simulated impacts of energetic electrons onto carbon nanotubes. We calculated the displacement threshold energies for carbon atoms in SWNTs or equivalently, shells of MWNTs with different diameters and chiralities. We showed that the displacement energy and the defect production rate depend on the diameter of the nanotubes and its chirality, and that for nanotubes with diameters less than 1 nm, the displacement energy is lower than the commonly accepted value. This stresses the importance of special care when investigating carbon nanotubes with small diameters by the transmission electron microscope. The calculated dependence of the atom displacement energy and tube diameter makes it possible to correlate the experimental information on the tube diameter to the maximum microscope voltage which can be used without creating any damage to the tube. We also calculated the displacement energies for carbon atoms near defects and showed that if a single vacancy is formed, it will likely be transformed to a double vacancy, as in this case the atomic network has no energetically unfavorable undercoordinated atoms. Thus mostly double vacancies will remain in the nanotube atomic network after high-dose electron irradiation. Overall, our results should help one to better understand electron-irradiation-induced transformations in carbon and B—C—N nanosystems,[34] and outline the most promising directions of electron-beam-mediated engineering of nanocarbon structures.

ACKNOWLEDGMENTS

The authors acknowledge support from the electron microscopy center Mainz (EMZM). The research was also supported by the Academy of Finland under Project Nos. 48751, 50578, and 202737, the Academy of Finland Center of Excellence Program (2000-2005), and partially by the ELENA project within the Academy of Finland TULE program. Grants of computer time from the Center for Scientific Computing in Espoo, Finland are gratefully acknowledged.

[1] M. Terrones, F. Banhart, N. Grobert, J.-C. Charlier, H. Terrones, and P. M. Ajayan, Phys. Rev. Lett. **89**, 075505 (2002).
[2] M. Terrones, H. Terrones, F. Banhart, J.-C. Charlier, and P. M. Ajayan, Science **288**, 1226 (2000).
[3] A. Kis, G. Csányi, J.-P. Salvetat, T.-N. Lee, E. Couteau, A. J. Kulik, W. Benoit, J. Brugger, and L. Fórro, Nat. Mater. **3**, 153 (2004).
[4] J. A. Aström, A. V. Krasheninnikov, and K. Nordlund, Phys. Rev. Lett. **93**, 215503 (2004).
[5] C.-H. Kiang, W. A. Goddard, R. Beyers, and D. S. Bethune, J. Phys. Chem. **100**, 3749 (1996).
[6] V. H. Crespi, N. G. Chopra, M. L. Cohen, A. Zettl, and S. G. Louie, Phys. Rev. B **54**, 5927 (1996).
[7] N. G. Chopra, F. M. Ross, and A. Zettl, Chem. Phys. Lett. **256**, 241 (1996).
[8] F. Banhart, T. Füller, P. Redlich, and P. M. Ajayan, Chem. Phys. Lett. **269**, 349 (1997).
[9] P. M. Ajayan, V. Ravikumar, and J.-C. Charlier, Phys. Rev. Lett. **81**, 1437 (1998).
[10] B. W. Smith and D. E. Luzzi, J. Appl. Phys. **90**, 3509 (2001).
[11] A. Hashimoto, K. Suenaga, A. Gloter, K. Urita, and S. Iijima, Nature (London) **430**, 870 (2004).
[12] K. Urita, K. Suenaga, T. Sugai, H. Shinohara, and S. Iijima, Phys. Rev. Lett. **94**, 155502 (2005).
[13] F. Banhart, J. X. Li, and A. V. Krasheninnikov, Phys. Rev. B **71**, 241408(R) (2005).
[14] F. Banhart, Rep. Prog. Phys. **62**, 1181 (1999).
[15] D. Porezag, T. Frauenheim, T. Köhler, G. Seifert, and R. Kaschner, Phys. Rev. B **51**, 12947 (1995).
[16] T. Frauenheim, G. Seifert, M. Elstner, T. Niehaus, C. Köhler, M. Amkreutz, M. Sternberg, Z. Hajnal, A. Di Carlo, and S. Suhai, J. Phys.: Condens. Matter **14**, 3015 (2002).
[17] A. V. Krasheninnikov, K. Nordlund, P. O. Lehtinen, A. S. Foster, A. Ayuela, and R. M. Nieminen, Phys. Rev. B **69**, 73402 (2004).
[18] P. O. Lehtinen, A. S. Foster, Y. Ma, A. V. Krasheninnikov, and R. M. Nieminen, Phys. Rev. Lett. **93**, 187202 (2004).
[19] G. Kresse and J. Furthmüller, Phys. Rev. B **54**, 11169 (1996).
[20] A. J. Lu and B. C. Pan, Phys. Rev. Lett. **92**, 105504 (2004).
[21] See EPAPS Document No. E-PRBMDO-72-010536 for animations showing the dynamics of the nanotube atoms after impacts of electrons with various energies. This document can be reached via a direct link in the online article's HTML reference section or via the EPAPS homepage (http://www.aip.org/pubservs/epaps.html).
[22] A. J. Stone and D. J. Wales, Chem. Phys. Lett. **128**, 501 (1986).
[23] Q. Zhao, M. B. Nardelli, and J. Bernholc, Phys. Rev. B **65**, 144105 (2002).
[24] P. Jensen, J. Gale, and X. Blase, Phys. Rev. B **66**, 193403 (2002).
[25] Y. Miyamoto, A. Rubio, S. Berber, M. Yoon, and D. Tománek, Phys. Rev. B **69**, 121413(R) (2004).
[26] A. V. Krasheninnikov and K. Nordlund, Nucl. Instrum. Methods Phys. Res. B **216**, 355 (2004).
[27] W. A. McKinley and H. Feshbach, Phys. Rev. **74**, 1759 (1948).
[28] T. D. Yuzvinsky, A. M. Fennimore, W. Mickelson, C. Esquivias, and A. Zettl, Appl. Phys. Lett. **86**, 053109 (2005).
[29] A. V. Krasheninnikov, K. Nordlund, and J. Keinonen, Phys. Rev. B **65**, 165423 (2002).
[30] S. L. Mielke, D. Troya, S. Zhang, J. L. Li, S. Xiao, R. Car, R. S. Ruoff, G. C. Schatz, and T. Belytschko, Chem. Phys. Lett. **390**, 413 (2004).
[31] S. Zhang, S. L. Mielke, R. Khare, D. Troya, R. S. Ruoff, G. C. Schatz, and T. Belytschko, Phys. Rev. B **71**, 115403 (2005).
[32] G. Gómez-Navarro, P. J. De Pablo, J. Gómez-Herrero, B. Biel, F. J. Garcia-Vidal, A. Rubio, and F. Flores, Nat. Mater. **4**, 534 (2005).
[33] F. Banhart, J. X. Li, and M. Terrones, Small (to be published).
[34] D. Golberg and Y. Bando, Recent Res. Dev. Phys. **2**, 1 (1999).